ECOLOGY LETTERS

Ecology Letters, (2013) doi: 10.1111/ele.12136

LETTER

Evolution of dispersal and life history interact to drive accelerating spread of an invasive species

T. Alex Perkins,[1*] Benjamin L. Phillips,[2] Marissa L. Baskett[1,3] and Alan Hastings[1,3]

Abstract

Populations on the edge of an expanding range are subject to unique evolutionary pressures acting on their life-history and dispersal traits. Empirical evidence and theory suggest that traits there can evolve rapidly enough to interact with ecological dynamics, potentially giving rise to accelerating spread. Nevertheless, which of several evolutionary mechanisms drive this interaction between evolution and spread remains an open question. We propose an integrated theoretical framework for partitioning the contributions of different evolutionary mechanisms to accelerating spread, and we apply this model to invasive cane toads in northern Australia. In doing so, we identify a previously unrecognised evolutionary process that involves an interaction between life-history and dispersal evolution during range shift. In roughly equal parts, life-history evolution, dispersal evolution and their interaction led to a doubling of distance spread by cane toads in our model, highlighting the potential importance of multiple evolutionary processes in the dynamics of range expansion.

Keywords

Climate shift, integral projection model, integrodifference equation, invasion front, invasion lag phase, natural selection, quantitative genetics, *Rhinella marina*, spatial selection, spatial spread.

Ecology Letters (2013)

INTRODUCTION

There is a growing appreciation that rapid evolution can alter ecological processes in important ways (e.g., Ellner *et al.* 2011; Schoener 2011). Rapid adaptation, for example, can change population dynamics in managed fisheries (Law 2000) and fundamentally alter disease dynamics (Ewald 1994). The rate at which a species shifts its range is another ecological process for which rapid evolution is increasingly seen as important. Predicting a species' rate of range shift has long been a major focus of ecologists (e.g. Elton 1958), because the magnitude of damage caused by noxious invasive species is determined by the speed and extent to which these species spread (Epanchin-Niell & Hastings 2010). Range shift is also critical to our understanding of how species track climate change: both historical climate change (Skellam 1951; Clark 1998) as well as the rapid anthropogenic shifts we are currently experiencing (Parmesan & Yohe 2003). Thus, a full understanding of the drivers of range expansion is an imperative for applied ecological research, and rapid evolution may well be an important facet of that understanding.

A phenomenon of interest in any range expansion is the possibility of increasing spread rates over time. Accelerating spread has been observed in many invasions (Veit & Lewis 1996; Crooks & Soule 1999; Urban *et al.* 2008), and four purely ecological mechanisms – long-distance dispersal, Allee effects, density-dependent dispersal and temporal variability – have been invoked to account for this phenomenon (Kot *et al.* 1996; Veit & Lewis 1996; Shigesada & Kawasaki 1997; Ellner & Schreiber 2012). An additional, evolutionary, explanation has also been proposed. This evolutionary explanation builds on the well-established principle that spread rate is determined jointly by population growth and dispersal at the invasion front (Fisher 1937) and argues that evolved changes in either dispersal or the life-history traits governing population growth can cause accelerating spread (Holt *et al.* 2005).

We might expect life-history and dispersal traits to evolve during spread for three related reasons. First, dispersal phenotypes are spatially assorted on the invasion front – only the best dispersers are represented at the leading edge of the front – and this leads to assortative mating by dispersal (Shine *et al.* 2011). Second, because the leading edge of the invasion front is at low density relative to populations behind it, individuals at the edge may experience little competition from conspecifics and so have high absolute fitness relative to individuals in the core of the range. Together, spatial assortment and the increased fitness of invasion-front individuals drive the evolution of increasing dispersal on the leading edge of the invasion front: an interaction of evolutionary forces that has been termed 'spatial selection' (Phillips *et al.* 2008b, 2010b). Third, life-history traits of populations at the edge can evolve in response to natural selection in the traditional sense. That is, life-history phenotypes that result in greater contributions to population growth under low-density conditions at the invasion front will be represented more among future occupants of the invasion front, wherever that may be (Holt *et al.* 2005; Phillips 2009; Perkins 2012).

Recent theoretical work has shown that these evolutionary forces can all generate phenotype change at the edge of an expanding range, that this change gives rise to accelerating spread, and that the extent of spread acceleration observed in nature can be achieved with modest heritabilities and realistic levels of selection (Travis & Dytham 2002; Travis *et al.* 2005, 2009; Burton *et al.* 2010; Bénichou *et al.* 2012; Bouin *et al.* 2012; Perkins 2012). This theoretical work has meanwhile been corroborated by numerous empirical demonstrations of evolved phenotypic changes in range-shifting popula-

[1]Center for Population Biology, University of California, Davis, CA,USA
[2]Centre for Tropical Biodiversity and Climate Change, School of Marine and Tropical Biology, James Cook University, Townsville, Qld, Australia
[3]Department of Environmental Science and Policy, University of California, Davis, CA,USA
*Correspondence: E-mail: taperkins@ucdavis.edu

tions (Rogers & Siemann 2004; Simmons & Thomas 2004; Phillips *et al.* 2006; 2008a; Hughes *et al.* 2007; Léotard *et al.* 2009; Phillips 2009) and the implication that such phenotype changes have resulted in accelerating spread in at least one case (Phillips *et al.* 2008a). Despite these multiple lines of evidence, an empirical link between trait evolution and accelerating spread has yet to be made.

This linkage is necessary because it is currently not known the extent to which accelerating spread is derived from rapid evolution in real-world examples. Further, we currently have no idea as to the relative roles of evolution of traits with direct impacts on population growth (hereafter 'life-history traits') vs. those directly related to dispersal (hereafter 'dispersal traits') in driving accelerating spread. Analyses of stage-structured integrodifference equations (Neubert & Caswell 2000; Caswell *et al.* 2003; Jongejans *et al.* 2008) and spatial integral projection models (Jongejans *et al.* 2011) show that shifts in either life-history or dispersal traits can impact spread rates, but these analyses do not account for the evolutionary processes that may or may not have led to those differences.

To integrate the three evolutionary forces outlined above and quantify their potential contributions to spread, we propose a general model that combines the well-known theories of stage-structured population dynamics, integrodifference equations and evolutionary quantitative genetics. The structure of this model is necessarily more complex than other quantitative-genetic models employed for the study of spatial phenomena in evolutionary ecology (e.g. Kirkpatrick & Barton 1997), because those models do not have the capacity for dispersal evolution (although see Bénichou *et al.* 2012; Bouin *et al.* 2012). At the same time, the model we propose is more easily parameterised with data and makes less specific assumptions than individual-based models (e.g. Burton *et al.* 2010). The resulting model is complex but can nonetheless be parameterised using commonly measured data: life tables, dispersal kernels, phenotype distributions and heritabilities. Here, we apply this model to the well-studied cane toad invasion of Australia, for which data to parameterise the model are readily available.

The cane toad (*Rhinella marina*) was first introduced in northeastern Australia in 1935. Since then it has spread to occupy more than 1.3 million km^2 of the continent (Urban *et al.* 2007). Importantly, while toads initially spread at around 10 km year^{-1}, their spread rate across northern Australia has steadily increased so that they now spread at around 50 km year^{-1} (Urban *et al.* 2008; Phillips *et al.* 2006). Furthermore, life-history evolution and dispersal evolution have both been documented in the toads' invasion across northern Australia (Phillips *et al.* 2006, 2008a, 2010b; Phillips 2009), and contemporary estimates of the phenotype distributions of two life-history traits (tadpole stage duration, metamorph growth) and one dispersal trait (dispersal distance) are available from near the introduction site (Gordonvale) and at a more recently invaded population (Timber Creek).

The confluence of these observations affords us a unique opportunity to place our analysis of the relative contributions of different evolutionary processes to spatial spread in an empirical context. Initialising the model with phenotypes from the introduction site, we compare phenotype evolution and distance spread after 72 years under model scenarios with differing assumptions about trait heritability. Examining differences in phenotype distributions and distance spread between model scenarios allows us to isolate the relative effects of the evolution of life-history vs. dispersal traits. Under our model, evolutionarily derived increases in cane toad spread are driven roughly equally by life-history evolution, dispersal evolution and, unexpectedly, by an interaction between the two. Combined, these evolutionary processes more than double distance spread in the model.

METHODS

Methodological overview

We developed a model with the specific intent of examining distance spread under different evolutionary scenarios. Our objective was not to determine how close different evolutionary scenarios came to emulating the observed spread of toads, but to understand the relative impacts of different evolutionary mechanisms on the joint dynamics of phenotype change and spatial spread. We realised different evolutionary scenarios by setting initial heritabilities either to zero or to some realistic positive value. The model was parameterised wherever possible with data, and initial heritabilities were selected such that the model produced changes in phenotype means close to differences between contemporary estimates of phenotype means in populations located near the introduction site (Gordonvale) and at a more recently invaded area (Timber Creek).

The variables

The model we use is designed to describe the dynamics of population densities, continuous genotype distributions and continuous phenotype distributions of multiple life stages in discrete time and continuous space. A general framework for modelling such dynamics for any collection of traits and an arbitrary categorisation of life stages is presented in the Supporting Information. The following description pertains to an application of that framework to cane toads.

Population densities of cane toad juveniles $J_t(x)$ and adults $A_t(x)$ are censused once per year t along a single spatial dimension x. These densities are further distributed across values of three quantitative traits: duration of the tadpole stage (T), metamorph growth rate (M) and dispersal tendency (D). Due to how they enter the model, we sometimes refer to T and M together as 'life-history traits' (L) and to D as the 'dispersal trait'.

Also at each time t and location x, the model follows the joint probability distributions, $\psi_{J,t}(\mathbf{g}, x)$ and $\psi_{A,t}(\mathbf{g}, x)$, of genotypes, $\mathbf{g} = (g_T, g_M, g_D)$, defined on the same scales of measurement as the traits themselves. At the onset of an invasion, we assume that these genotypes are multivariate normally distributed about their means with additive genetic variance $\mathbf{G}$. The bearers of each genotype combination possess phenotypes, $\mathbf{z} = (z_T, z_M, z_D)$, that are multivariate normally distributed with mean equal to their genotype value and variance $\mathbf{E}$ attributable to various environmental and non-additive genetic sources. Consequently, joint phenotype distributions, $\psi_{J,t}(\mathbf{z}, x)$ and $\psi_{A,t}(\mathbf{z}, x)$, are also multivariate normally distributed with variance $\mathbf{P} = \mathbf{G} + \mathbf{E}$ at the onset of invasion. Thereafter, all genotype and phenotype distributions are free to depart from their initial forms due to selection and gene flow. The initial heritability of trait i, h_i^2, is then equal to $\mathbf{G}_{i,i}/\mathbf{P}_{i,i}$. We con-

strained all covariances between traits to zero, although the modelling framework is flexible in this regard.

The model

We now describe the biological assumptions and processes governing the spatiotemporal dynamics of the aforementioned variables for cane toads. A detailed mathematical exposition of the general modelling framework and additional information about the numerical implementation of the cane toad model are available in the Supporting Information.

For the population-dynamic component of the model, we apply an existing model of cane toad population dynamics (Lampo & De Leo 1998) at local populations along the spatial dimension x. Per capita recruitment to the juvenile stage is a product of clutch size ϕ, egg survival σ_E, tadpole survival σ_T and metamorph survival σ_M (Fig. 1, top left). Survivals through the tadpole and metamorph stages are not fixed, however (Fig. 1, top). Assuming constant daily mortality risks for tadpoles and metamorphs, survival through each of these stages depends on how long it takes for toads to progress through them. Accordingly, maximal survival through the tadpole stage under ideal conditions can be written as

$$\hat{\sigma}_T(z_T) = \hat{\sigma}_{T,\text{daily}}^{z_T}, \tag{1}$$

where $\hat{\sigma}_{T,\text{daily}}$ is maximal daily survival. Consistent with Lampo & De Leo (1998), we define realised survival through the tadpole stage as a density-dependent function

$$\sigma_T(z_T) = \frac{\hat{\sigma}_T(z_T)}{1 + dT}, \tag{2}$$

where d is the strength of density dependence and $T = \phi\sigma_E A$ is tadpole density. The metamorph phenotype, on the other hand, is

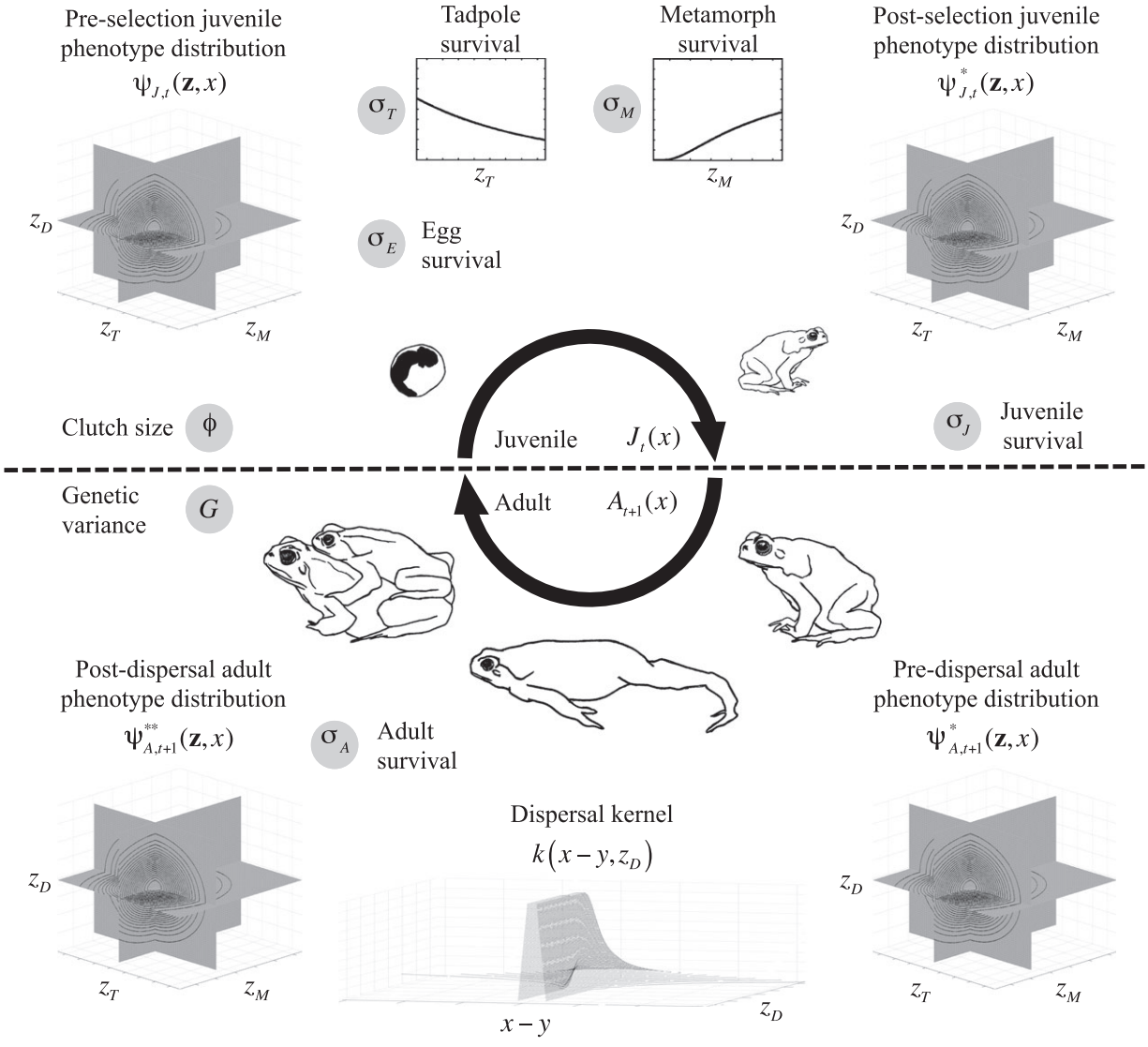

Figure 1. Model schematic showing the progression of the cane toad life cycle (clockwise) through the juvenile (top) and adult (bottom) stages. The four slice plots of the $\mathbf{z} = (z_T, z_M, z_D)$ phenotype space at some point in space x show the distinct phenotype distributions tracked by our model: $\psi_{J,t}(\mathbf{z},x)$ (top left) is that of a virgin cohort; $\psi^*_{J,t}(\mathbf{z},x)$ (top right) results from phenotype-dependent tadpole and metamorph survival; $\psi^*_{A,t+1}(\mathbf{z},x)$ (bottom right) comprises newly matured adults and those surviving from past years; $\psi^{**}_{A,t+1}(\mathbf{z},x)$ (bottom left) is the result of phenotype-dependent dispersal from and to each location. Model parameters are highlighted with grey backgrounds.

defined as a growth rate. By stipulating that passage through the metamorph stage requires some critical amount of growth, we can calculate the survival of a metamorph with a relatively fast or slow growth rate by raising baseline metamorph survival $\tilde{\sigma}_M$ to a power of the ratio of the baseline growth rate $\tilde{z}_M$ with that individual's growth rate z_M; i.e.

$$\sigma_M(z_M) = \tilde{\sigma}_M^{\tilde{z}_M/z_M}. \quad (3)$$

After surviving those preliminary stages, a proportion σ_J of juveniles survives to adulthood in the second year (Fig. 1, right), and a proportion σ_A of adults survives to each year thereafter (Fig. 1, bottom).

The dynamics of local populations distributed along the spatial dimension x are linked by a dispersal event each year. We assume that juveniles do not move far enough to be of any consequence at a geographical scale, so we only model dispersal explicitly for adults. The outcome of this dispersal event is governed by a probability density function $k(x, x')$ that determines how a population at each location x' redistributes itself to all other locations x. We implement dispersal with a kernel that depends on the distance $|x - x'|$ between locations and on an individual's dispersal phenotype z_D (Fig. 1, bottom).

Phenotype-dependent survival and dispersal in the model allow for the possibility of genetically based evolution, provided that there is variation among genotypes (i.e. any entry of $\mathbf{G}>0$). Because our model specifies the relationship between the distributions of phenotypes and the genotypes that underlie them, we can directly calculate how phenotype-dependent survival and dispersal shape the genotype distributions, $\psi_{J,t}(\mathbf{g}, x)$ and $\psi_{A,t}(\mathbf{g}, x)$. Following selection on juveniles, maturation to adulthood and adult dispersal, adult toads mate randomly to produce the distribution of genotypes that will enter the juvenile cohort in the following year (Fig. 1, left). The full mathematical form of the model can be reproduced by applying the preceding details to the general model formulation presented in the Supporting Information.

Parameterisation

Distributions of life-history phenotypes in our model were parameterised by fitting normal distributions to the relevant subset of the values of z_T and z_M measured in Phillips (2009) (Fig. 2, bottom left and centre). Specifically, we used phenotype measurements from juveniles reared in a common laboratory environment whose parents were collected *in situ* near either Gordonvale or Timber Creek and then bred in a common laboratory environment (Phillips 2009). Thus, there is strong evidence that the differences between the distributions of z_T and z_M between these populations are genetic in origin. The fitted distributions from offspring of toads collected near Gordonvale served as the initial conditions of these distributions in our model at the onset of invasion. Likewise, the fitted distributions from offspring of toads collected near Timber Creek served as the empirical benchmark against which the life-history phenotypes in our model were compared after 72 years of spread. Values of all other parameters in the population-dynamic component of the model were taken from Lampo & De Leo (1998).

The dispersal component of the model was parameterised using radiotracking data from Phillips *et al.* (2008a). The subset of toads from that study that we used here was collected *in situ* near either Gordonvale or Timber Creek and held in a common environment for two months. Thereafter, toads were released at a common location in the field and radiotracked for five nights, rendering a list of daily movement distances and turning angles for each released individual. This experimental design ensured that environmental effects at the time of observation were controlled for, and a subsequent study (Phillips *et al.* 2010a) demonstrated a clear genetic basis to differences between the populations at Gordonvale and Timber Creek. To then obtain a distribution of displacements over 180 days (the approximate length of the active season for toads in northern Australia), we summed 180 resampled daily movements for each toad 10^5 times. Assuming that daily movements are independent and identically distributed for each individual, the sum of daily movements over the course of a season should converge to a normal distribution. With the further assumption that movements were isotropic, and thus that there was zero mean displacement, each individual's normal dispersal kernel has a single variance parameter σ^2 that determines the scale of its dispersal. Finding that these individual variances are approximately lognormally distributed, we defined the dispersal phenotype as $z_D = \log(\sigma^2)$ to obtain a normally distributed dispersal phenotype appropriate for our model. The distribution of z_D at the onset of invasion was then parameterised by fitting a normal distribution to all $\log(\sigma^2)$ of toads collected near Gordonvale (Fig. 2, bottom right). Likewise, the normal distribution of z_D fitted to all $\log(\sigma^2)$ of toads collected near Timber Creek served as the empirical benchmark against which the dispersal phenotype in our model was compared after 72 years of spread (Fig. 2, bottom right).

The evolutionary component of our model was parameterised by setting the initial heritability of each trait to the value that resulted in a change in phenotype mean after 72 years equal to the difference between phenotype means measured at Gordonvale and Timber Creek (Fig. 2, bottom). For the life-history traits, we picked initial heritabilities that satisfied this criterion given a simplified model of phenotype change in which selection at the invasion front was assumed to remain consistent for the very small population size that defined the location of the moving invasion front (details available in the Supporting Information). Because no simpler model of dispersal evolution in this context is possible, we used the full model to pick an initial heritability for the dispersal trait consistent with the difference between phenotype means at Timber Creek and Gordonvale. This resulted in the following values for the initial heritabilities: $h_T^2 = 0.10$, $h_M^2 = 0.16$ and $h_D^2 = 0.21$.

Analysis

Our primary aim was to determine the relative contributions of natural selection (on life-history) vs. spatial selection (on dispersal) as drivers of phenotypic change and spread acceleration on moving invasion fronts. To determine the consequences of different scenarios in which these factors play varying roles, we compared phenotype means at the invasion front and distances spread after 72 years under different scenarios. The four scenarios we examined allowed neither, either, or both sets of traits to evolve by manipulating which traits had a positive initial heritability. Hereafter, we will refer to these scenarios using the convention L_0D_0, L_+D_0, L_0D_+ and L_+D_+, where the subscripts of L denote the positivity of both h_T^2 and h_M^2, and the subscripts of D denote the positivity of h_D^2. Positive values of initial heritabilities were consistent across scenarios.

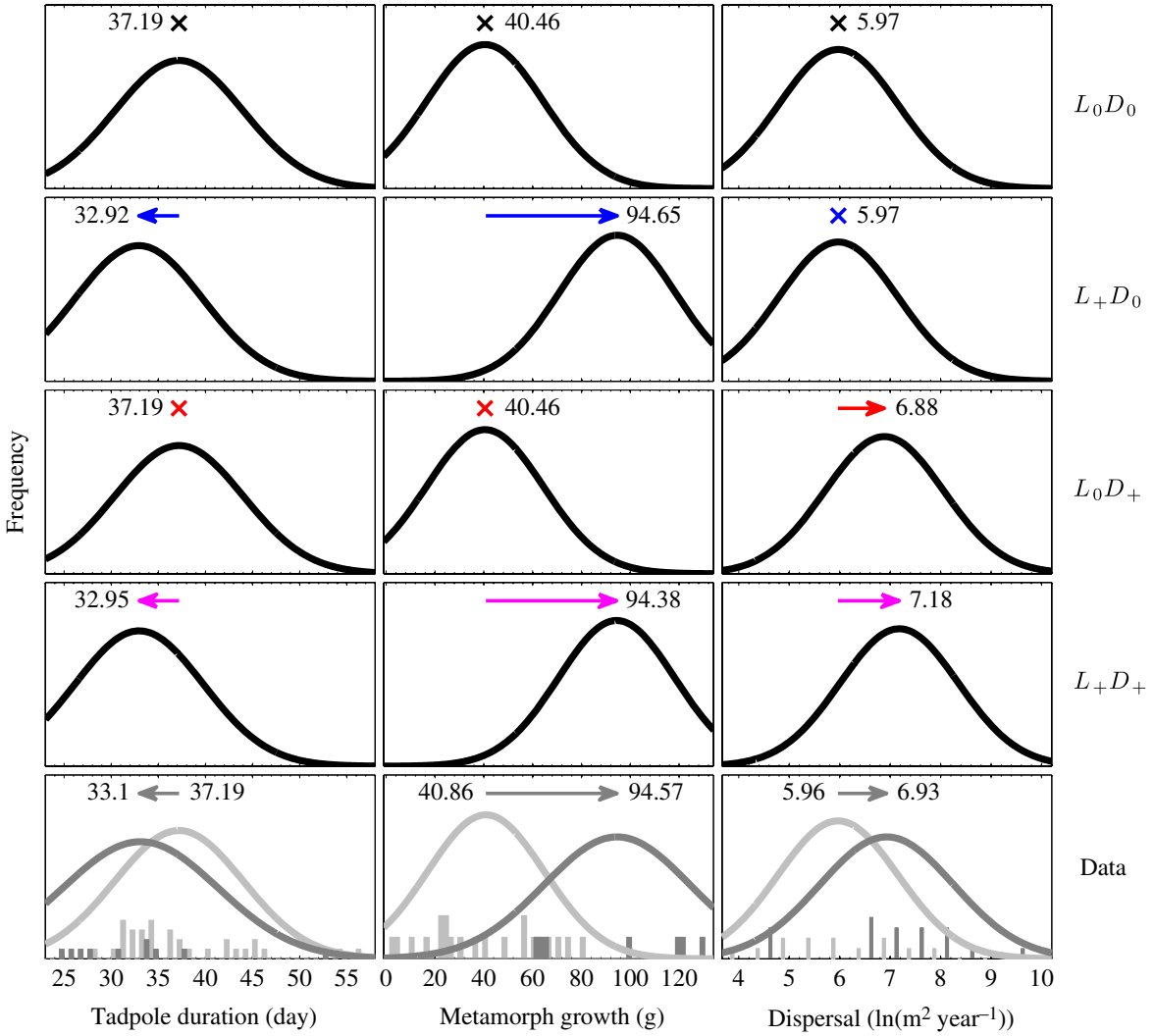

Figure 2. Phenotype marginal distributions of tadpole duration (left column), metamorph growth (centre column) and dispersal tendency (right column), estimated from empirical data from Gordonvale (bottom row, light grey) and Timber Creek (bottom row, dark grey) and calculated with our model under different scenarios (top four rows) about initial heritability of life-history (L) and dispersal (D) traits (0, not heritable; +, heritable). Arrows show direction and magnitude of difference in phenotype means between Gordonvale and Timber Creek, and their colours correspond to the scenarios in Fig. 3. A × indicates no change in phenotype mean.

RESULTS

Allowing traits to evolve led to substantial improvements in the model's ability to reproduce the phenomenon of accelerating spread observed by Urban *et al.* (2008). In the absence of genetic variation and evolution (L_0D_0), spread in the model proceeded at a constant rate to a distance of 470 km after 72 years (Fig. 3). Thus, the best available data indicate that variable but non-evolving dispersal is not sufficient to account for the accelerating spread of toads. Evolution of life-history and dispersal traits, run separately, increased distance spread to 601 km (L_+D_0) and 677 km (L_0D_+) respectively. When life-history and dispersal traits were allowed to evolve simultaneously (L_+D_+), spread accelerated markedly to a distance of 1004 km (Fig. 3): a 114% increase in distance spread relative to the scenario with no evolution.

Another important, and more general, result to emerge is that the extent to which traits evolve in the model is not consistent across scenarios. In particular, when all phenotypes were allowed to evolve independently in scenario L_+D_+, the life-history traits fell slightly short of their final values achieved in the L_+D_0 scenario, but the dispersal trait greatly exceeded the value it achieved in the L_0D_+ scenario (Fig. 2). The fact that the dispersal trait changed much more in L_+D_+ than in L_0D_+ implies an interaction between life-history and dispersal evolution during spread. Such an interaction can be explained by an increase in the strength of spatial selection acting on the dispersal trait. Because both spatial sorting and natural selection interact to drive the evolution of dispersal during spread (together, spatial selection), when population growth increases due to natural selection the rate of dispersal evolution also increases. This 'enhanced spatial selection' strongly impacts the dispersal trait because of the gradient in that trait along the invasion front driven by spatial sorting. The distributions of the life-history traits, on the other hand, show no such gradient (because these phenotypes are not associated with dispersal distance) and so do not receive the additional evolutionary boost afforded to dispersal.

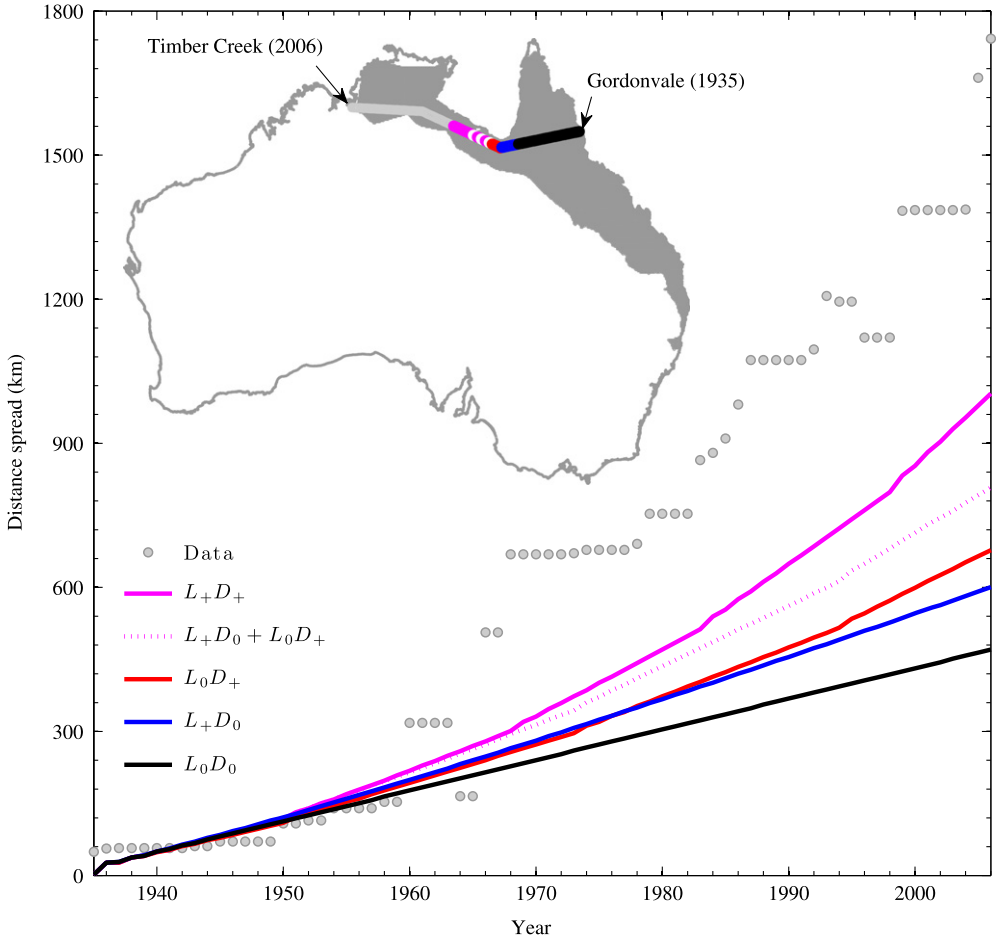

Figure 3. Distance spread by cane toads, modelled under different evolutionary scenarios. Solid lines correspond to model scenarios about initial heritabilities (0 or +) of life-history (L) and dispersal (D) traits. The dashed line shows the sum of the increases in distance spread in scenarios in which only one type of trait evolved (L_+D_0 and L_0D_+) relative to when neither evolved (L_0D_0), which contrasts with the scenario in which both traits evolved simultaneously (L_+D_+). The line between Gordonvale and Timber Creek shows the one-dimensional path along which spread was modelled, and colours on that line show distance spread by 2006 under the different model scenarios. Although the model was neither fit to spread data nor intended to fully recreate empirical patterns, we show an empirical estimate of cane toads' distance spread over time and their range in Australia as of 2006 for context (from Urban *et al.* 2008).

Finally, the scenarios we examined allow us to partition the spread increase in L_+D_+ relative to L_0D_0 into contributions from natural selection on life-history traits (24%), spatial selection on the dispersal trait (39%) and enhanced spatial selection on the dispersal trait that occurred as a by-product of the evolution of the life-history traits and their impact on population growth (37%). Thus, changes in the dispersal trait were directly responsible for most (76%) of the increase in spread due to evolution, but nearly half of that increase was an indirect result of life-history evolution. The acceleration of cane toad spread in our model therefore appears not to have been dominated by any single trait or evolutionary process.

DISCUSSION

Although previous work has demonstrated genetically based evolution of cane toads (Phillips *et al.* 2006, 2008b, 2010a; Phillips 2009) and suggested that these changes might have accounted for accelerating spread across northern Australia (Phillips *et al.* 2006, 2008a), ours is the first study to connect these disparate data on phenotype change and spatial spread with a mathematical model. Our results show that modest heritabilities (0.10–0.21) are sufficient to account for phenotype changes between the introduction site and the invasion front (Fig. 2) and that these changes have large enough effects on population growth and dispersal to have a substantial impact on spread on the ecological time scale of interest (Fig. 3). By comparing phenotype changes and distances spread under different scenarios about the initial heritability of life-history and dispersal traits, we found that no single evolving trait dominated spread dynamics. Rather, life-history evolution, dispersal evolution and an interaction between the two all appear to have made important contributions to the spatial spread of this invasive species. In particular though, the increase in spread due to an interaction between life-history and dispersal evolution identifies a new mechanism, which we term 'enhanced spatial selection', for trait change during spread and highlights the importance of this process for the spread of invasive species.

The process of enhanced spatial selection would seem to be a general outcome of allowing both life history and dispersal to evolve during spread. If we recall that spatial selection on dispersal is the interaction between spatial assortment of dispersal phenotypes and differential population growth driven by density release, then we can see that higher population growth resulting from natural

selection should indeed enhance spatial selection. More generally, any factor that modulates a gradient in population growth in the direction of spread has the potential to modulate dispersal evolution, enhancing or suppressing it depending on the direction of the gradient. For a species spreading into increasingly inhospitable conditions (e.g. to track a shifting climate), the action of spatial selection could be suppressed. Indeed, even without an environmental gradient, spatial selection can be suppressed by Allee effects (Travis & Dytham 2002). Together, however, our model and the body of evidence for cane toads suggest that natural selection on life-history traits enhanced the evolution of dispersal traits in the cane toad invasion of northern Australia.

Moreover, the various mechanisms for trait change during range expansion are not simply evolutionary curiosities but also drivers of ecological dynamics. In the case of the cane toad invasion of northern Australia, our analysis posits that genetically based trait change could have led to a more than twofold increase in the distance spread by cane toads over 72 years. This impact on spread appears equally attributable to three distinct mechanisms: natural selection, spatial selection and enhanced spatial selection. In other systems, the contributions of these mechanisms will likely differ from those seen here, depending on patterns of genetic variation and selection. In related but strictly ecological analyses, some have shown that differences in demographic characteristics contribute more to differences in spread rates (Caswell *et al.* 2003; Smith *et al.* 2009), whereas others have shown that differences in dispersal play a larger role (Caswell *et al.* 2003; Bullock *et al.* 2008; Jongejans *et al.* 2008). Although we are unable to provide general answers about when certain ecological or evolutionary mechanisms contribute more or less to spread, we do make the important advance of demonstrating the impact that rapid evolution can have on spread in a natural system and discovering the importance of an interaction between life-history and dispersal evolution. By building on our modelling framework (i.e. applying it to other species or developing novel extensions of it), others will be able to provide additional clarity on these issues.

Although our model is well supported by empirical studies and well suited to assessing the relative impacts of different evolutionary scenarios on spread, it should not be misconstrued as an attempt to thoroughly recreate the spread dynamics of cane toads. Most notably, the distance spread in our most plausible evolutionary scenario was only 58% of the empirical estimate of distance spread by Urban *et al.* (2008). This is unsurprising for several reasons, of which we comment on a few. First, and perhaps most importantly, spatial spread is an inherently stochastic process that is extremely difficult to predict, even in controlled laboratory environments (Melbourne & Hastings 2009). Second, any number of factors not considered by our model could have affected spread, including spatiotemporal variability (Grosholz 1996), genotype-by-environment interactions (Bowler & Benton 2005), and subtle environmental gradients (Urban *et al.* 2008). Incorporating such factors would likely only affect absolute predictions of the model rather than relative predictions across evolutionary scenarios, which are our focus. Third, more exhaustive sampling of daily displacements by Phillips *et al.* (2008a) or assuming a leptokurtic form of the individual dispersal kernel could have led to much greater estimates of distance spread, but doing so would not be supported by available evidence and would not impact our findings. Despite these limitations, our analysis is clear about the relative impacts of different evolutionary mechanisms on spread, and it yields quantitative results about distance spread on the same order of magnitude as empirical estimates.

Our analysis should also not be construed as a complete recreation of the evolutionary history of cane toads in Australia. One source of uncertainty is that, for lack of historical evidence, we initialise phenotypes in the model based on contemporary estimates from Gordonvale and thus assume that the population there has evolved very little. The behaviour of the model at the introduction site contradicts this assumption, however. With all $h_i^2 > 0$, changes in $\overline{z}_T$, $\overline{z}_M$, and $\overline{z}_D$ at the introduction site equal 76, 84 and 4% of the changes at the invasion front. This assumption of little change at the introduction site is therefore appropriate for dispersal evolution but less so for life-history evolution. Rather than bend the model to accommodate this behaviour by calibrating initial phenotype distributions and heritabilities to potentially unrealistic values, we find a more parsimonious reconciliation of this discrepancy to be that the model of life-history evolution is simply less appropriate for the high-density context of an established population than it is for a low-density population on the invasion front (Phillips *et al.* 2010b). Although further empirical studies of life-history evolution in the wild could provide clarity on this issue, such refinements would have little bearing on our qualitative results about the impact of different evolutionary forces on the dynamics of frontal populations. Another source of uncertainty is the evolutionary impact of a secondary introduction sometime around 1964–1968 in an area about 150 km ahead of the invasion front (Estoup *et al.* 2004). Joint analysis of genetic data and historical distribution records, however, indicates relatively little signal of this secondary introduction in the genetics of descendent populations (Estoup *et al.* 2010). Incorporating this secondary introduction into our model may therefore have little impact on our estimates of evolution along the invasion front but could boost our estimate of distance spread.

Perhaps the most serious limiting assumption of our model is that about genetic variation. Our model does allow for changes in genetic variation due to selection and gene flow and for departures of the genotype distributions from normality (Turelli & Barton 1994). It does not, however, account for changes in genetic variation due to drift. Even so, because we calibrated trait heritabilities to achieve empirically estimated shifts in trait means, allowing for a decay in heritability over time due to drift would have simply required a recalibration of our initial heritability estimates. The main consequence of this is that the initial heritability values that we used could somewhat under-represent the true heritabilities during the early stages of the cane toad's invasion. In addition to genetic variation within traits, our modelling framework is also capable of accommodating genetic covariances among traits, but we have no such data for cane toads and likely will not for some time due to the difficulty of fully estimating the **G** matrix for non-model organisms. Despite these uncertainties, our model accords with empirical demonstrations that life-history and dispersal traits in cane toads are heritable and that they have shifted during the cane toad's rapid range expansion across northern Australia (Phillips *et al.* 2006, 2008a, 2010a; Phillips 2009).

CONCLUSION

Overall, we have developed a useful framework with which to explore the role of evolution in the ecological dynamics of range

expansion. Applying this framework to cane toads, our results indicate that rapid evolution of life-history and dispersal traits at the invasion front could have led to a more than twofold increase in the distance spread by cane toads across northern Australia. Additionally, by partitioning evolutionary impacts on spread into those acting separately on life-history and dispersal traits, our analysis reveals a new mechanism for dispersal evolution under range shift: enhanced spatial selection. These results speak broadly to the importance of incorporating the capacity for trait change into spread models and into ecological models more generally. Doing so can have dramatic impacts on the predictions flowing from such models and thereby on our capacity to anticipate and manage the dynamics of species undergoing range shifts during invasion or in response to climate change.

ACKNOWLEDGEMENTS

TAP received funding from a Computational Sciences Graduate Fellowship, which is managed by Krell Institute under contract No. DE-FG02-97ER25308 with the US Department of Energy. BLP was supported by the Australian Research Council's Fellowships programme. We thank S.J.E. Baird for helpful discussions about how to model dispersal, M. Turelli for comments on an earlier draft of this manuscript, M. Perkins for drawing toads for Fig. 1, and M. Urban for supplying code to generate the map in Fig. 3.

AUTHORSHIP

TAP and BLP conceived of the study. All authors contributed to the model's development, and TAP performed the analyses. TAP and BLP wrote the first draft of the manuscript, and all authors contributed substantially to revisions.

REFERENCES

Bénichou, O., Calvez, V., Meunier, N. & Voituriez, R. (2012). Front acceleration by dynamic selection in Fisher population waves. *Phys. Rev. E*, 86, 041908.

Bouin, E., Calvez, V., Meunier, N., Mirrahimi, S., Perthame, B., Raoul, G. & Voituriez, R. *et al.* (2012). Invasion fronts with variable motility: phenotype selection, spatial sorting and wave acceleration. *Comptes Rendus Mathematique*, 350, 761–766.

Bowler, D.E. & Benton, T.G. (2005). Causes and consequences of animal dispersal strategies: relating individual behaviour to spatial dynamics. *Biol. Rev.*, 80, 205–225.

Bullock, J.M., Pywell, R.F. & Coulson-Phillips, S.J. (2008). Managing plant population spread: prediction and analysis using a simple model. *Ecol. Appl.*, 18, 945–953.

Burton, O.J., Phillips, B.L. & Travis, J.M.J. (2010). Trade-offs and the evolution of life-histories during range expansion. *Ecol. Lett.*, 13, 1210–1220.

Caswell, H., Lensink, R. & Neubert, M.G. (2003). Demography and dispersal: life table response experiments for invasion speed. *Ecology*, 84, 1968–1978.

Clark, J.S. (1998). Why trees migrate so fast: confronting theory with dispersal biology and the paleorecord. *Am. Nat.*, 152, 204–224.

Crooks, J.A. & Soule, M.E. (1999). Lag times in population explosions of invasive species: causes and implications. In: *Invasive Species and Biodiversity Management* (eds. Sandlund, O.T., Schei, P.J. & Viken, A.). Kluwer Academic Publishers, The Netherlands, chap. 7, pp. 103–125.

Ellner, S.P., Geber, M.A. & Hairston, N.G. (2011). Does rapid evolution matter? Measuring the rate of contemporary evolution and its impacts on ecological dynamics. *Ecol. Lett.*, 14, 603–614.

Ellner, S.P. & Schreiber, S.J. (2012). Temporally variable dispersal and demography can accelerate the spread of invading species. *Theor. Popul. Biol.*, 82, 283–298.

Elton, C.S. (1958). *The ecology of invasions by animals and plants*. Methuen, London.

Epanchin-Niell, R.S. & Hastings, A. (2010). Controlling established invaders: integrating economics and spread dynamics to determine optimal management. *Ecol. Lett.*, 13, 528–541.

Estoup, A., Baird, S.J., Ray, N., Currat, M., Cornuet, J.M., Santos, F., Beaumont, M.A. *et al.* (2010). Combining genetic, historical and geographical data to reconstruct the dynamics of bioinvasions: application to the cane toad *Bufo marinus*. *Mol. Ecol. Resour.*, 10, 886–901.

Estoup, A., Beaumont, M., Sennedot, F., Moritz, C. & Cornuet, J.M. (2004). Genetic analysis of complex demographic scenarios: spatially expanding populations of the cane toad, *Bufo marinus*. *Evolution*, 58, 2021–2036.

Ewald, P.W. (1994). *Evolution of Infectious Disease*. Oxford University Press, New York.

Fisher, R. (1937). The wave of advance of advantageous genes. *Ann. Hum.Genet.*, 7, 355–369.

Grosholz, E.D. (1996). Contrasting rates of spread for introduced species in terrestrial and marine systems. *Ecology*, 77, 1680–1686.

Holt, R.D., Barfield, M. & Gomulkiewicz, R. (2005). Theories of niche conservatism and evolution: could exotic species be potential tests? In: *Species Invasions: Insights into Ecology, Evolution, and Biogeography* (eds. Sax, D. F., Stachowicz, J.J. & Gaines, S.D.). Sinauer, Sunderland, MA, pp. 259–290.

Hughes, C.L., Dytham, C. & Hill, J.K. (2007). Modelling and analysing evolution of dispersal in populations at expanding range boundaries. *Ecol. Entomol.*, 32, 437–445.

Jongejans, E., Shea, K., Skarpaas, O., Kelly, D. & Ellner, S. (2011). Importance of individual and environmental variation for invasive species spread: a spatial integral projection model. *Ecology*, 92, 86–97.

Jongejans, E., Shea, K., Skarpaas, O., Kelly, D., Sheppard, A.W. & Woodburn, T.L. (2008). Dispersal and demography contributions to population spread of *Carduus nutans* in its native and invaded ranges. *J. Ecol.*, 96, 687–697.

Kirkpatrick, M. & Barton, N.H. (1997). Evolution of a species' range. *Am. Nat.*, 150, 1–23.

Kot, M., Lewis, M.A. & van den Driessche, P. (1996). Dispersal data and the spread of invading organisms. *Ecology*, 77, 2027–2042.

Lampo, M. & De Leo, G.A. (1998). The invasion ecology of the toad *Bufo marinus*: from South America to Australia. *Ecol. Appl.*, 8, 388–396.

Law, R. (2000). Fishing, selection, and phenotypic evolution. *ICES J. Mar. Sci.*, 57, 659–668.

Léotard, G., Debout, G., Dalecky, A., Guillot, S., Gaume, L., McKey, D. & Kjellberg, F. *et al.* (2009). Range expansion drives dispersal evolution in an equatorial three-species symbiosis. *PLoS ONE.*, 4, e5377.

Melbourne, B.A. & Hastings, A. (2009). Highly variable spread rates in replicated biological invasions: fundamental limits to predictability. *Science*, 325, 1536–1539.

Neubert, M.G. & Caswell, H. (2000). Demography and dispersal: calculation and sensitivity analysis of invasion speed for structured populations. *Ecology*, 81, 1613–1628.

Parmesan, C. & Yohe, G. (2003). A globally coherent fingerprint of climate change impacts across natural systems. *Nature*, 421, 37–42.

Perkins, T.A. (2012). Evolutionarily labile species interactions and spatial spread of invasive species. *Am. Nat.*, 179, E37–E54.

Phillips, B.L. (2009). The evolution of growth rates on an expanding range edge. *Biol. Lett.*, 5, 802–804.

Phillips, B.L., Brown, G.P. & Shine, R. (2010a). Evolutionarily accelerated invasions: the rate of dispersal evolves upwards during the range advance of cane toads. *J. Evol. Biol.*, 23, 2595–2601.

Phillips, B.L., Brown, G.P. & Shine, R. (2010b). Life-history evolution in range-shifting populations. *Ecology*, 91, 1617–1627.

Phillips, B.L., Brown, G.P., Travis, J.M.J. & Shine, R. (2008a). Reid's paradox revisited: the evolution of dispersal kernels during range expansion. *Am. Nat.*, 172, 34–48.

Phillips, B.L., Brown, G.P., Webb, J.K. & Shine, R. (2006). Invasion and the evolution of speed in toads. *Nature*, 439, 803.

Phillips, B.L., Chipperfield, J.D. & Kearney, M.R. (2008b). The toad ahead: challenges of modelling the range and spread of an invasive species. *Wildl. Res.*, 35, 222.

Rogers, W.E. & Siemann, E. (2004). Invasive ecotypes tolerate herbivory more effectively than native ecotypes of the Chinese tallow tree *Sapium sebiferum*. *J. Appl. Ecol.*, 41, 561–570.

Schoener, T.W. (2011). The newest synthesis: understanding the interplay of evolutionary and ecological dynamics. *Science*, 331, 426–429.

Shigesada, N. & Kawasaki, K. (1997). *Biological Invasions: Theory and Practice*. Oxford University Press, Oxford.

Shine, R., Brown, G.P. & Phillips, B.L. (2011). An evolutionary process that assembles phenotypes through space rather than through time. *Proc. Natl. Acad. Sci.*, 108, 8–11.

Simmons, A.D. & Thomas, C.D. (2004). Changes in dispersal during species' range expansions. *Am. Nat.*, 164, 378–395.

Skellam, J.G. (1951). Random dispersal in theoretical populations. *Biometrika*, 38, 196–218.

Smith, C.A., Giladi, I. & Lee, Y.S. (2009). A reanalysis of competing hypotheses for the spread of the California sea otter. *Ecology*, 90, 2503–2512.

Travis, J.M.J. & Dytham, C. (2002). Dispersal evolution during invasions. *Evol. Ecol. Res.*, 4, 1119–1129.

Travis, J.M.J., Hammershoj, M. & Stephenson, C. (2005). Adaptation and propagule pressure determine invasion dynamics: insights from a spatially explicit model for sexually reproducing species. *Evol. Ecol. Res.*, 7, 37–51.

Travis, J.M.J., Mustin, K., Benton, T.G. & Dytham, C. (2009). Accelerating invasion rates result from the evolution of density-dependent dispersal. *J. Theor. Biol.*, 259, 151–158.

Turelli, M. & Barton, N.H. (1994). Genetic and statistical analyses of strong selection on polygenic traits: what, me normal? *Genetics*, 138, 913–941.

Urban, M.C., Phillips, B.L., Skelly, D.K. & Shine, R. (2007). The cane toad's (*Chaunus* [*Bufo*] *marinus*) increasing ability to invade Australia is revealed by a dynamically updated range model. *Proc. R. Soc. B: Biol. Sci.*, 274, 1413–1419.

Urban, M.C., Phillips, B.L., Skelly, D.K. & Shine, R. (2008). A toad more traveled: the heterogeneous invasion dynamics of cane toads in Australia. *Am. Nat.*, 171, E134–E148.

Veit, R.R. & Lewis, M.A. (1996). Dispersal, population growth, and the Allee effect: dynamics of the house finch invasion of eastern North America. *Am. Nat.*, 148, 255–274.

SUPPORTING INFORMATION

Additional Supporting Information may be downloaded via the online version of this article at Wiley Online Library (www.ecologyletters.com).

Editor, John Fryxell
Manuscript received 18 December 2012
First decision made 28 January 2013
Second decision made 9 April 2013
Manuscript accepted 12 May 2013

Supporting Information for

Evolution of dispersal and life history interact to drive accelerating spread of an invasive species

T. Alex Perkins[1,*], Benjamin L. Phillips[2], Marissa L. Baskett[1,3], Alan Hastings[1,3]

[1] Center for Population Biology, University of California, Davis, CA, USA

[2] Centre for Tropical Biodiversity and Climate Change, School of Marine and Tropical Biology, James Cook University, Townsville Australia

[3] Department of Environmental Science and Policy, University of California, Davis, CA, USA

∗ E-mail: taperkins@ucdavis.edu

Contents

1 Description of the general model

1.1 Overview

Here we present a general model for the simultaneous population and evolutionary dynamics of a stage-structured species distributed over a continuous stretch of space. This model is similar to the spatial integral projection model put forth by Jongejans *et al.* (2011) but with the addition of 1) quantitative genetics machinery to incorporate selection on and inheritance of the species' traits, and 2) the specification of dispersal kernel parameters as quantitative traits that are heritable and variable among individuals (after Petrovskii & Morozov, 2009; Petrovskii *et al.*, 2011).

1.2 Local dynamics

Consider a well-mixed population in which individuals utilize the same pool of resources and encounter each other randomly and repeatedly. Individuals fall into discrete classes according to age or life stage. Moreover, individuals are variable in one or more phenotypes. The quantities that capture ecologically relevant variation in the population are thus the distribution $\mathbf{n}$ of abundance among stages and the joint density ψ of m phenotypes $z_1, ..., z_m \in \mathbf{z}$. Transitions of $\mathbf{n}$ from one stage to another via survival or reproduction occur once per year t.

Although this setting could pertain to a variety of traits, we focus on continuously measurable traits such as body size or growth rate. Underlying such quantitative phenotypes $\mathbf{z}$ are breeding values $\mathbf{g}$, which are continuously measurable genotypes defined on the same scales of measurement as the phenotypes. Assuming that each breeding value is the sum of identically small contributions from a very large number of unlinked loci, the infinitesimal model of quantitative genetics posits that the joint distribution of m genotypes is multivariate normal (MVN) over $\mathbf{g}$ with mean μ and an m-by-m additive genetic covariance matrix $\mathbf{G}$ (Bulmer, 1971, 1976). For a set of m traits not under selection, the joint breeding value distribution (JBVD) is defined mathematically as

$$\psi(\mathbf{g}) = \text{MVN}(\mathbf{g}, \mu, \mathbf{G}) = \frac{1}{(2\pi)^{\frac{m}{2}}|\mathbf{G}|^{\frac{1}{2}}} \exp\left(-\frac{1}{2}(\mathbf{g}-\mu)'\mathbf{G}^{-1}(\mathbf{g}-\mu)\right). \tag{S1}$$

The primary reason to model the full JBVD in the first place is if selection or gene flow is strong enough to cause $\psi(\mathbf{g})$ to depart from $\text{MVN}(\mathbf{g}, \mu, \mathbf{G})$. Thus, we initialize $\psi(\mathbf{g})$ as in eq. (S1) but allow it to depart from the MVN assumption in subsequent generations.

Selection ultimately results in changes to the JBVD, but it is the joint phenotype distribution (JPD) on which selection acts. The relationship between the JBVD and the JPD is a constant source of random variation encapsulated by the covariance matrix $\mathbf{E}$. This variation may be due to either non-additive genetic or environmental sources, and, like the JBVD, the JPD is also MVN. The heritability h^2 of each trait specifies the relationship between $\mathbf{G}$ and $\mathbf{E}$ (i.e., $h_i^2 = \mathbf{G}_{i,i}/\left(\mathbf{G}_{i,i} + \mathbf{E}_{i,i}\right)$) and thus how phenotypic variation is partitioned between additive genetic and environmental sources, assuming there are no genotype-by-environment interactions.

Selection on phenotypes enters the model whenever transition rates between stages are phenotype-dependent. Transitions to stage 0 involve reproduction at a rate $a_{i,0}$ that is defined as the per-capita number of offspring produced per time step. Transitions to all other stages $j \neq 0$ involve survival at rate $a_{i,j}$. In both cases, the transition rate can be written as a function $a_{i,j}(\mathbf{z})$ of phenotype $\mathbf{z}$, which results in demographic contributions from stage i to stage j of

$$n^*_{i\to j,t} = n_{i,t} \int a_{i,j}(\mathbf{z})\psi_{i,t}(\mathbf{z})d\mathbf{z} \tag{S2}$$

and a JPD contribution of

$$\psi^*_{i\to j,t}(\mathbf{z}) = \frac{a_{i,j}(\mathbf{z})\psi_{i,t}(\mathbf{z})}{\int a_{i,j}(\mathbf{z})\psi_{i,t}(\mathbf{z})d\mathbf{z}}, \tag{S3}$$

where $\int d\mathbf{z}$ represents a multiple integral $\int_{\mathbb{R}^m} dz_1 \cdots dz_m$. For survival transitions to stages $j \neq 0$, the abundance of stage j at time step $t+1$ is then the sum of contributions from all other stages,

$$n_{j,t+1} = \sum_i n^*_{i\to j,t}, \tag{S4}$$

and the JPD of stage j at time step $t+1$ is the weighted average

$$\psi_{j,t+1}(\mathbf{z}) = \frac{\sum_i n^*_{i\to j,t}\psi^*_{i\to j,t}(\mathbf{z})}{\int \sum_i n^*_{i\to j,t}\psi^*_{i\to j,t}(\mathbf{z})d\mathbf{z}} \tag{S5}$$

of contributions from all other stages following the transition.

Transitions to stage 0, which involve reproduction within and among reproductive stages R, are somewhat different. First, the JBVD must be recovered from the JPD. This can be achieved by performing a deconvolution of the JPD of each reproductive stage to remove variation attributable to the MVN distribution defined by $\mathbf{E}$. Then, assuming that mating is random within and among reproductive stages, the JBVD of the gamete pool is the weighted average

$$\psi^{**}_t(\mathbf{g}) = \frac{\sum_{i\in R} n^*_{i\to 0,t}\psi^*_{i\to 0,t}(\mathbf{g})}{\int \sum_{i\in R} n^*_{i\to 0,t}\psi^*_{i\to 0,t}(\mathbf{g})d\mathbf{g}} \tag{S6}$$

of breeding value contributions $\psi^*_{i\to 0,t}(\mathbf{g})$ from all reproductive stages $i \in R$ to the gamete pool. The JBVD of zygotes in the next time step $t+1$ is then the product of the JBVD of the gamete pool with itself and the conditional probability $L(\mathbf{g}|\mathbf{g}_1, \mathbf{g}_2)$ that parents with JBVs $\mathbf{g}_1$ and $\mathbf{g}_2$ have offspring with JBV $\mathbf{g}$, all of which is expressed mathematically as

$$\psi_{0,t+1}(\mathbf{g}) = \int\int L(\mathbf{g}|\mathbf{g}_1, \mathbf{g}_2)\psi^{**}_t(\mathbf{g}_1)\psi^{**}_t(\mathbf{g}_2)d\mathbf{g}_1 d\mathbf{g}_2 \tag{S7}$$

(Slatkin, 1970; Karlin, 1979). Assuming there is no variation in fecundity, $L(\mathbf{g}|\mathbf{g}_1, \mathbf{g}_2)$ can be defined to equal MVN($\mathbf{g}$, $\frac{\mathbf{g}_1+\mathbf{g}_2}{2}$, $\frac{\mathbf{G}}{2}$) (Turelli & Barton, 1994), where the genic variance $\frac{\mathbf{G}}{2}$ is the portion of the additive genetic variance that is unperturbed by gametic-phase disequilibrium due to selection (Walsh, 2003). The assumption of identical fecundity among parents also simplifies the dynamics of the stage-0 abundance at the beginning of time step $t+1$, which are the same as in eq. (S4) with $j = 0$ and $i \in R$.

1.3 Spatial dynamics

To explore population dynamics distributed over a geographic scale, which is required to study spatial spread, it is necessary to model multiple populations coupled by dispersal. We assume a continuum of populations arranged along a single spatial dimension, such as a coastline or a habitat corridor. For the sake of generality to other landscapes, the extension of results from spread models on a single spatial dimension to a two-dimensional landscape is straightforward as long as movement is isotropic (i.e., the same in all directions); the spread of a one-dimensional range is equivalent to the spread rate of the range radius of an analogous population defined in two dimensions (Lewis *et al.*, 2006).

Just as phenotype variation may generate variation in survival or reproduction, so too may it lead to variable dispersal patterns among individuals in a population. Dispersal of individuals with dispersal phenotype z_d occurs according to a stage- and phenotype-dependent dispersal kernel $k_i(|x-y|; z_d)$, which is a probability density function over space that specifies the probability that an individual with phenotype z_d disperses to a location of distance $|x-y|$ away from where it started. In our definition of k, the dispersal kernel parameter z_d is synonymous with the dispersal phenotype. In reality, however, the kernel parameter is likely to be a function of one or more underlying phenotypes. Even so, in the absence of a known relationship between the kernel parameter and one or more biologically grounded phenotypes, we treat the two as the same.

Given the discrete nature of events in our model, dispersal must be defined to occur at some point in a sequence with reproduction and survival. We proceed by assuming that dispersal occurs last in this sequence, although the model could easily be adapted to an alternative order of events for application to other species. For each of the dispersing stages D, the spatial distribution of abundance after dispersal is given by the convolution of the spatial distribution of abundance after selection and before dispersal ($n^*_{i\to j,t}(x)$) with the average kernel

$$k_{i,y}(|x-y|) = \int k_i(|x-y|; z_d)\psi^*_{i,t}(z_d, y)dz_d, \tag{S8}$$

at y weighted across the dispersal phenotypes after selection and before dispersal ($\psi^*_{i,t}(z_d, y)$), resulting in

$$n_{j,t+1}(x) = \sum_{\forall i \in D} \int k_{i,y}(|x-y|) n^*_{i\to j,t}(y) dy. \tag{S9}$$

The spatial JPD after dispersal follows the same pattern of spatial rearrangement as abundance. That is, the JPD at location x after dispersal,

$$\psi_{j,t+1}(\mathbf{z}, x) = \frac{\sum_{i\in D} \int k_i(|x-y|; z_d) n^*_{i\to j,t}(y) \psi^*_{i\to j,t}(\mathbf{z}, y) dy}{\int \sum_{i\in D} \int k_i(|x-y|; z_d) n^*_{i\to j,t}(y) \psi^*_{i\to j,t}(\mathbf{z}, y) dy d\mathbf{z}}, \tag{S10}$$

is influenced most by the JPDs from locations that are nearby ($|x-y|$ small) and abundant ($n^*_{i\to j,t}$ large). The spatial JPD of stage-0 individuals after dispersal is the same as in eq. (S10) except that the right-hand side of eq. (S7) is substituted for $\psi^*_{i\to j,t}(\mathbf{z}, y)$.

2 Numerical implementation of the model

2.1 Discretization

One necessary step in numerically implementing a model with continuous variables is discretizing them. To strike a balance between too coarse a discretization that model behavior was changed and too fine a discretization that the program exceeded our computer's memory capacity, we discretized space into approximately 2000 points evenly spaced between 0 and 3000 km from the invasion source. The JBVD of the three traits was modeled by a 25^3-element array ranging the phenotype mean plus or minus three phenotypic standard deviations of each trait. We shifted the JBVD array each time step such that the mean of each trait was always at the center of the array.

2.2 Invasion front

We defined the invasion front as the farthest point from the invasion source where the number of adults exceeded one one-hundredth of their equilibrium density as defined by Lampo & De Leo (1998). To conserve memory, we modeled JBVD dynamics only within a window around the invasion front of width twice the 98^{th}-percentile dispersal distance of toads with dispersal phenotypes equal to the mean plus three standard deviations. To determine whether our results were robust to the size of the window around the invasion front, we also evaluated the model with windows twice the 90^{th}- and 95^{th}-percentile dispersal distances of those toads. We found that the greatest departure from the results we present is that 90^{th}-percentile windows increased CDS after 72 years by 20 km, relative to a 98^{th}-percentile window, because of a smaller distance between discretized populations. Because of this relatively small effect, we used 98^{th}-percentile dispersal distances in our analyses.

2.3 Selection on breeding values

A feature of the model that posed more serious numerical challenges was the transition from eq. (S6) to eq. (S7), which required deconvolution of environmental variation from the JPD to obtain the JBVD. To avoid numerical instabilities introduced by deconvolution, we cast all evolutionary dynamics in terms of breeding values rather than phenotypes. The primary change this necessitated was revising functions for phenotype-dependent survival and dispersal to apply directly to breeding values.

As noted by Lande (1979, eq. 4), the mean fitness of breeding values, $\tilde{W}(\mathbf{g})$, can be calculated by taking the expectation of the fitness of phenotypes, $W(\mathbf{z})$, weighted by the distribution of phenotypes about each breeding value, $\mathrm{MVN}(\mathbf{z}, \mathbf{g}, \mathbf{E})$, resulting in

$$\tilde{W}(\mathbf{g}) = \int W(\mathbf{z}) \, \mathrm{MVN}(\mathbf{z}, \mathbf{g}, \mathbf{E}) \, d\mathbf{z}. \tag{S11}$$

Likewise, this procedure can be applied to transform other functions of $\mathbf{z}$ into functions of $\mathbf{g}$, such as those in eqq. (S2), (S3), (S5), (S8), and (S10). Doing so obviates the need to perform a deconvolution to extract $\psi(\mathbf{g})$ from $\psi(\mathbf{z})$ following selection and dispersal and prior to mating. Most importantly, the evolutionary and demographic dynamics resulting from such an implementation of the model are identical to those that would result from implementing eqq. (S2), (S3), (S5), (S8), and (S10) directly on phenotypes.

A potential limitation of this approach is that after one round of selection on a virgin cohort, the transformation in eq. (S11) may no longer be accurate because the differential survival of phenotypes without respect to their breeding values erodes the MVN relationship between them. With this limitation in mind, we applied the transformation in eq. (S11) only once on each trait over the lifetime of a cohort. Thus, our numerical results are consistent with the general modeling framework presented herein.

3 Estimating heritabilities of the life-history traits

To calibrate h_T^2 and h_M^2, we used a simplified model of phenotype change to ensure that our heritability estimates were influenced only by natural selection at a stable wavefront (as in Perkins, 2012). In doing so, any differences between phenotype change in the full and simplified models can be attributed to complications beyond those explicit in the formulation of the simplified model.

The assumptions of the simplified model are as follows. First, we assume that a stable wavefront moves along a single spatial dimension x at instantaneous speed $c(t)$ at time t. We define the point on the wavefront moving at this speed to be that at which the local density of adults equals $\alpha\hat{A}$, where α is some small proportion and $\hat{A}$ is the equilibrium density of adults in a closed population. Second, we assume that local population dynamics can be modeled as in Lampo & De Leo (1998), with the refinement that σ_T and σ_M depend on z_T and z_M as specified in eqq. (1)-(3). Third, we assume that adults disperse once per time step according to a normal kernel, and that individuals do not vary in their propensity to disperse. Under these assumptions, the temporal dynamics of z_T and z_M at the invasion front can be approximated by the equations governing their dynamics in a closed population (Perkins, 2012, eq. C1).

Simplified dynamics of multiple phenotype means at the invasion front can then be modeled using eq. 7a of Lande (1979). Under this formulation, per-generation changes $\Delta\overline{z}_T$ and $\Delta\overline{z}_M$ of phenotype means follow

$$\begin{bmatrix} \Delta\overline{z}_T \\ \Delta\overline{z}_M \end{bmatrix} = \mathbf{G} \begin{bmatrix} \frac{\partial}{\partial\overline{z}_T} \ln \overline{R}_0 \\ \frac{\partial}{\partial\overline{z}_M} \ln \overline{R}_0 \end{bmatrix}, \tag{S12}$$

where $\mathbf{G}$ is the genetic covariance matrix and $\overline{R}_0$ is mean per-capita per-generation population growth. Given phenotype means of $\overline{z}_T(0)$ and $\overline{z}_M(0)$ at time 0, the values of phenotype means at time N can be found by iterating

$$\begin{bmatrix} \overline{z}_T(t+1) \\ \overline{z}_M(t+1) \end{bmatrix} = \begin{bmatrix} \overline{z}_T(t) \\ \overline{z}_M(t) \end{bmatrix} + \begin{bmatrix} \Delta\overline{z}_T \\ \Delta\overline{z}_M \end{bmatrix} \tag{S13}$$

N times.

Although the model in eqq. (S12) and (S13) can project dynamics of phenotype means given arbitrary $\mathbf{G}$, we define this matrix in a particular way for the purpose of estimating heritabilities:

$$\mathbf{G} = \begin{bmatrix} h_T^2 V_{P,T} & 0 \\ 0 & h_M^2 V_{P,M} \end{bmatrix}. \tag{S14}$$

The traits are therefore genetically independent, but, as we will see, their dynamics are linked because they each impact the strength of selection on the other.

To calculate selection gradients, we first make the simplifying assumption that

$$\overline{R}_0\left(z_T, z_M\right) = R_0\left(\overline{z}_T, \overline{z}_M\right), \tag{S15}$$

and note the equivalence

$$\frac{\partial \ln R_0}{\partial \overline{z}} = \frac{1}{R_0}\frac{\partial R_0}{\partial \overline{z}}. \tag{S16}$$

We therefore need to calculate per-capita per-generation population growth R_0 and its partial derivatives with respect to each phenotype mean. Given the projection matrix

$$\begin{bmatrix} 0 & F \\ \sigma_J & \sigma_A \end{bmatrix}, \tag{S17}$$

per-capita per-generation population growth is given by

$$R_0 = \sum_{i=1}^{\infty} F\sigma_J\sigma_A^i \tag{S18}$$

$$= \frac{F\sigma_J}{1-\sigma_A} \tag{S19}$$

(Caswell, 2000). Dependence of R_0 on mean phenotypes enters eq. (S19) via per-female juvenile recruitment F, defined as

$$F = \frac{\phi}{2}\sigma_E\sigma_T\sigma_M, \tag{S20}$$

through dependencies of σ_T and σ_M on $\overline{z}_T$ and $\overline{z}_M$.

The expression for σ_M in terms of $\overline{z}_M$ is straightforward,

$$\sigma_M\left(\overline{z}_M\right) = \tilde{\sigma}_M^{\tilde{z}_M/\overline{z}_M}, \tag{S21}$$

with baseline metamorph survival $\tilde{\sigma}_M$ modified by the ratio of the baseline metamorph growth $\tilde{z}_M$ and mean metamorph growth $\overline{z}_M$ in the population at the invasion front. The expression for tadpole survival σ_T at the invasion front is more complicated, because it depends on tadpole density T, which in turn depends on adult density A. At the invasion front, we have defined adult density to equal $\alpha\hat{A}$, so tadpole density there will be $\frac{\phi}{2}\sigma_E\alpha\hat{A}$. Plugging this expression, an expression for $\hat{A}$ modified from Lampo & De Leo (1998), and the dependencies of $\hat{\sigma}_{T,daily}$ and $\tilde{\sigma}_M$ on $\overline{z}_T$ and $\overline{z}_M$ into the expression for σ_T gives

$$\sigma_T\left(\overline{z}_T, \overline{z}_M, \alpha\right) = \frac{\hat{\sigma}_{T,\mathrm{daily}}^{\overline{z}_T}}{(1-\alpha) + \alpha\frac{\frac{\phi}{2}\sigma_E\hat{\sigma}_{T,\mathrm{daily}}^{\overline{z}_T}\tilde{\sigma}_M^{\tilde{z}_M/\overline{z}_M}\sigma_J}{1-\sigma_A}}. \tag{S22}$$

Now that per-capita per-generation population growth R_0 and its dependencies on the $\overline{z}_T$ and $\overline{z}_M$ phenotype means have been made clear, we can calculate the selection gradients

$$\frac{\partial}{\partial \overline{z}_T} R_0\left(\overline{z}_T, \overline{z}_M, \alpha\right) = \frac{\sigma_J}{1-\sigma_A} \frac{\partial}{\partial \overline{z}_T} F\left(\overline{z}_T, \overline{z}_M, \alpha\right) \tag{S23}$$

$$\frac{\partial}{\partial \overline{z}_M} R_0\left(\overline{z}_T, \overline{z}_M, \alpha\right) = \frac{\sigma_J}{1-\sigma_A} \frac{\partial}{\partial \overline{z}_M} F\left(\overline{z}_T, \overline{z}_M, \alpha\right) \tag{S24}$$

by taking partial derivatives of eq. (S19). Selection, of course, depends critically on how juvenile recruitment varies with $\overline{z}_T$ and $\overline{z}_M$, which can be determined by taking more partial derivatives,

$$\frac{\partial}{\partial \overline{z}_T} F\left(\overline{z}_T, \overline{z}_M, \alpha\right) = \frac{\phi}{2} \sigma_E \sigma_M\left(\overline{z}_M\right) \frac{\partial}{\partial \overline{z}_T} \sigma_T\left(\overline{z}_T, \overline{z}_M, \alpha\right) \tag{S25}$$

$$\frac{\partial}{\partial \overline{z}_M} F\left(\overline{z}_T, \overline{z}_M, \alpha\right) = \frac{\phi}{2} \sigma_E \sigma_M\left(\overline{z}_M\right) \frac{\partial}{\partial \overline{z}_M} \sigma_T\left(\overline{z}_T, \overline{z}_M, \alpha\right) \tag{S26}$$

$$+ \frac{\phi}{2} \sigma_E \sigma_T\left(\overline{z}_T, \overline{z}_M, \alpha\right) \frac{\partial}{\partial \overline{z}_M} \sigma_M\left(\overline{z}_M\right) \tag{S27}$$

The last step in completing the expression for selection is determining how changes in $\overline{z}_T$ and $\overline{z}_M$ affect σ_T and σ_M. These last partial derivatives equal

$$\frac{\partial}{\partial \overline{z}_T} \sigma_T\left(\overline{z}_T, \overline{z}_M, \alpha\right) = \frac{\hat{\sigma}_{T,\text{daily}}^{\overline{z}_T} \ln\left(\hat{\sigma}_{T,\text{daily}}\right)}{(1-\alpha) + \alpha \frac{\frac{\phi}{2} \sigma_E \hat{\sigma}_{T,\text{daily}}^{\overline{z}_T} \tilde{\sigma}_M^{\tilde{z}_M/\overline{z}_M} \sigma_J}{1-\sigma_A}} \tag{S28}$$

$$- \frac{\alpha \frac{\frac{\phi}{2} \sigma_E \hat{\sigma}_{T,\text{daily}}^{2\overline{z}_T} \ln\left(\hat{\sigma}_{T,\text{daily}}\right) \tilde{\sigma}_M^{\tilde{z}_M/\overline{z}_M} \sigma_J}{1-\sigma_A}}{\left((1-\alpha) + \alpha \frac{\frac{\phi}{2} \sigma_E \hat{\sigma}_{T,\text{daily}}^{\overline{z}_T} \tilde{\sigma}_M^{\tilde{z}_M/\overline{z}_M} \sigma_J}{1-\sigma_A}\right)^2}, \tag{S29}$$

$$\frac{\partial}{\partial \overline{z}_M} \sigma_T\left(\overline{z}_T, \overline{z}_M, \alpha\right) = \frac{\alpha \frac{\frac{\phi}{2} \sigma_E \hat{\sigma}_{T,\text{daily}}^{2\overline{z}_T} \tilde{\sigma}_M^{\tilde{z}_M/\overline{z}_M} \ln\left(\tilde{\sigma}_M\right) \tilde{z}_M \sigma_J}{1-\sigma_A}}{\overline{z}_M^2 \left((1-\alpha) + \alpha \frac{\frac{\phi}{2} \sigma_E \hat{\sigma}_{T,\text{daily}}^{\overline{z}_T} \tilde{\sigma}_M^{\tilde{z}_M/\overline{z}_M} \sigma_J}{1-\sigma_A}\right)^2}, \tag{S30}$$

$$\frac{\partial}{\partial \overline{z}_M} \sigma_M\left(\overline{z}_M\right) = \frac{-\tilde{\sigma}_M^{\tilde{z}_M/\overline{z}_M} \ln\left(\tilde{\sigma}_M\right) \tilde{z}_M}{\overline{z}_M^2}. \tag{S31}$$

Given that we would like to know what values of h_T^2 and h_M^2 account for a given amount

of phenotype change over a number of *years* and the time step of our model is in *generations*, we must determine the length of a generation in years. Several definitions of generation length exist, but here we use the definition that generation length is

$$\Gamma = \frac{\ln R_0}{\ln \lambda}, \tag{S32}$$

where λ is per-capita per-year population growth and equals the dominant eigenvalue of the projection matrix in eq. (S17) (Caswell, 2000). It is important to note that the generation length will change as phenotypes evolve because R_0 and λ are functions of σ_T and σ_M.

Finally, to find values of h_T^2 and h_M^2 that account for phenotype change over 72 years, we ran the model in eq. (S13) until the cumulative sum of successive Γs exceeded 72. Doing so for all combinations of $h_T^2 \in \{0.01, 0.02, ..., 0.30\}$ and $h_M^2 \in \{0.01, 0.02, ..., 0.30\}$, we found that $h_T^2 = 0.10$ and $h_M^2 = 0.16$ produced $\overline{z}_T$ and $\overline{z}_M$ with the smallest mean percent difference from the phenotype means measured at Timber Creek. We therefore used these values in all of our analyses in which $h_T^2 > 0$ or $h_M^2 > 0$.

References

Bulmer, M. G. (1971). The effect of selection on genetic variability. *American Naturalist*, 105, 201–211.

Bulmer, M. G. (1976). Regressions between relatives. *Genetical Research*, 28, 199–203.

Caswell, H. (2000). *Matrix Population Models: Construction, Analysis, and Interpretation*. Sinauer Associates.

Jongejans, E., Shea, K., Skarpaas, O., Kelly, D. & Ellner, S. (2011). Importance of individual and environmental variation for invasive species spread: A spatial integral projection model. *Ecology*, 92, 86–97.

Karlin, S. (1979). Models of multifactorial inheritance. 1. Multivariate formulations and basic convergence results. *Theoretical Population Biology*, 15, 308–355.

Lampo, M. & De Leo, G. a. (1998). The invasion ecology of the toad *Bufo marinus*: From South America to Australia. *Ecological Applications*, 8, 388–396.

Lande, R. (1979). Quantitative genetic analysis of multivariate evolution, applied to brain : body size allometry. *Evolution*, 33, 402–416.

Lewis, M., Neubert, M., Caswell, H., Clark, J. & Shea, K. (2006). A guide to calculating discrete-time invasion rates from data. In: *Conceptual Ecology and Invasion Biology: Reciprocal Approaches to Nature*. Springer, pp. 169–192.

Perkins, T. A. (2012). Evolutionarily labile species interactions and spatial spread of invasive species. *American Naturalist*, 179, E37–E54.

Petrovskii, S., Mashanova, A. & Jansen, V. (2011). Variation in individual walking behavior creates the impression of a Lévy flight. *Proceedings of the National Academy of Sciences*, 108, 8704.

Petrovskii, S. & Morozov, A. (2009). Dispersal in a statistically structured population: Fat tails revisited. *American Naturalist*, 173, 278–89.

Slatkin, M. (1970). Selection and polygenic characters. *Proceedings of the National Academy of Sciences of the United States of America*, 66, 87–93.

Turelli, M. & Barton, N. H. (1994). Genetic and statistical analyses of strong selection on polygenic traits: What, me normal? *Genetics*, 138, 913–941.

Walsh, B. (2003). Evolutionary Quantitative Genetics. In: *Handbook of Statistical Genetics* (eds. Balding, D., Bishop, M. & Cannings, C.), vol. 23, 2nd edn., chap. 14. Wiley, pp. 389–442.